EUROPEAN ORGANIZATION FOR NUCLEAR RESEARCH

CERN/EP 88-124
23 September 1988

A SEARCH FOR GLUEBALLS IN THE CENTRAL REGION IN THE REACTION $pp \to p_f(X^0)p_s$ AT 300 GeV/c USING THE CERN Ω SPECTROMETER

WA76 Collaboration

Dedicated to the memory of our friend and colleague

Yves Goldschmidt-Clermont

T.A. Armstrong [4,*)], M. Benayoun [5)], W. Beusch [4)], I.J. Bloodworth [3)], M. Caponero [2)], J.N. Carney [3)], R. Childs [3)], B.R. French [4)], B. Ghidini [2)], Y. Goldschmidt-Clermont [4,7)], A. Jacholkowski [4)], J. Kahane [5)], J.B. Kinson [3)], A. Kirk [3)], K. Knudson [4)], V. Lenti [2)], Ph. Leruste [5)], A. Malamant [5)], J.L. Narjoux [5)], F. Navach [2)], A. Palano [2)], E. Quercigh [4)], N. Redaelli [4,**)], L. Rossi [4,***)], M. Sené [5)], R. Sené [5)], H.R. Shaylor [3)], M. Stassinaki [1)], M.T. Trainor [4)], G. Vassiliadis [1)], O. Villalobos Baillie [3)], M.F. Votruba [3)], G. Zito [2)] and R. Zitoun [6)]

1) Athens University, Physics Department, Athens, Greece
2) Dip. di Fisica dell'Università and Sez. INFN, Bari, Italy
3) University of Birmingham, Physics Department,Birmingham,U.K.
4) CERN, CH-1211 Geneva 23, Switzerland
5) Collège de France, Paris, France
6) LPNHE, Universités de Paris VI et VII, Paris, France
7) Deceased

Abstract

The aim of this experiment is to search for gluonic mesons in the reaction $pp \to p_f(X^0)p_s$ at 300 GeV/c incident proton momentum, where the X^0 system is a centrally produced meson. Preliminary results are presented on the two-body ($\pi^+\pi^-$, K^+K^-, $K^0_SK^0_S$, $p\bar{p}$), three body ($K^0_SK^\pm\pi^\mp$) and four-body ($2\pi^+2\pi^-$) decays of the X^0 system.

XXIV International Conference on High Energy Physics

Munich, August 4-10 1988

---

*) Present address: Pennsylvania State University, University Park, USA
**) Present address: INFN and Dip. di Fisica, Milan, Italy
***) Present address: INFN and Dip. di Fisica, Genoa, Italy

1. Introduction

The present understanding of strong interactions is that they are described by Quantum Chromo-Dynamics (QCD). This non-Abelian field theory not only describes how quarks and antiquarks interact, but also predicts that the gluons which are the quanta of the field will themselves interact to form mesons. If the object formed is composed entirely of valence gluons the meson is called a glueball, however if it is composed of a mixture of valence quarks, antiquarks and gluons (i.e. $q\bar{q}g$) it is called a hybrid. The search for these states has been carried out by studying several production mechanisms such as prompt production at high P_T [1], J/ψ radiative and hadronic decays [2], $p\bar{p}$ annihilations and central production [3] [4] [5].

Experiment WA76 is designed to study exclusive final states formed in the reaction

$$pp \rightarrow p_f(X^0)p_s \qquad (1)$$

where the subscripts f and s indicate the fastest and slowest particles in the laboratory respectively and X^0 represents the central system that is presumed to be produced by a double exchange processes. At high centre-of-mass energies these double exchange process are believed to be dominated by Double Pomeron Exchange (DPE), where the Pomeron is thought to have a large gluonic content, leading to the conclusion that Pomeron-Pomeron scattering could be a source of gluonic states. The expected features of DPE reactions are a slow growth in the cross section with increasing centre-of-mass energy [6], and the production of even spin resonances.

Experiment WA76 has been performed at two incident beam momenta, 85 and 300 GeV/c, corresponding to centre-of-mass energies of $\sqrt{s}$ = 12.7 and 23.8 GeV. Results from the 85 GeV/c run have been presented previously [5] and this paper deals with a preliminary analysis of $\approx$95 % of the 300 GeV/c data.

2. Layout of the Omega Spectrometer in experiment WA76

The experiment was performed at the CERN Omega Spectrometer, using the layout shown in fig.1. The trigger was designed to enhance double exchange processes with respect to single exchange and elastic processes.

The positively charged H1 beam in the West Area was incident on a 60 cm long hydrogen target. A set of four scintillation hodoscopes having a logical slab size of 0.33 mm and four 50 μm pitch μ-strip detectors were used to perform an accurate measurement of the incident beam's position and momentum which was held at 300 GeV/c with a momentum bite of ± 0.25 %.

The fast track, which had a momentum in the range 200 to 300 GeV/c, was measured by two sets of 4 μ-strip detectors placed 6 and 10 m downstream from the target. The standard Ω MWPC's and Drift Chambers were used to measure the medium momentum tracks ($\approx$ 1 to 40 GeV/c) leaving the interaction region.

The two threshold Cerenkov counters C1 and C2, with the associated hodoscope system where used for charged particle identification.

The trigger required

1. A fast particle defined by a hit in the counter A_1 (2.5×2.5 cm^2) placed after the Drift Chamber 2 (DC2) and a hit in the counter A_2 (5.0×5.0 cm^2) placed after Cerenkov C1. The A_1 and A_2 counters were the same size as the μ-strip planes and were placed very close to them.

2. A slow momentum ($<$ 1.0 GeV/c) particle defined by demanding a hit on one of the fourteen horizontal slabs of the Slow Proton Counter (SPC), a hit in the side of the box counter (TS) nearest to the SPC and $\geq$ 1 hits on a single plane of the MWPC's placed parallel to the target.

3. Target diffraction and excitation was reduced by requiring no hits in the other three sides of the scintillator box (TS) which surrounded the target.

4. To reduce forward diffraction no hit was requested in the two DFC counters (30×30 cm^2) which were placed on either side of the beam and just downstream of Cerenkov C1.

The layout was such that the fast track and the slow proton are always detected with a positive transverse momentum component (P_y). This acts as a veto on elastic events while enabling the study of events involving only neutral particles which can be detected by the gamma calorimeter. The total number of events recorded using this trigger was 12×10^6.

It is the aim of this paper to present preliminary results on the $\pi^+\pi^-$, K^+K^-, $K^0_SK^0_S$, $p\bar{p}$, $K^0_SK^\pm\pi^\mp$ and $\pi^+\pi^-\pi^+\pi^-$ central systems.

3. Selection of the Reaction $pp \rightarrow p_f(h\bar{h})p_s$

The reactions

$$pp \rightarrow p_f(h\bar{h})p_s,$$

where h = π, K or p,

have been isolated from the sample of events having four outgoing tracks by first imposing cuts on the components of missing momentum (|missing P_z| < 0.08 GeV/c, |missing P_y| < 0.16 GeV/c, |missing P_x| < 20 GeV/c).

Fig.2a shows the total missing P_T where a clear signal of candidate "4C" events can be seen. Fig.2b shows the resulting longitudinal missing momentum after placing a cut on the missing P_T. These plots show that momentum balance events can clearly be isolated and therefore that exclusive physics can be done at 300 GeV/c incident beam momentum.

The slow particle is identified as a slow proton by applying a cut to the pulse heights in the SPC and the TS as a function of momentum.

In order to select a given central system the Ehrlich mass [7], shown in fig.3a, is plotted for all the 4-prong events which balance momentum. The distribution peaks at the square of the π mass which is the signal of the centrally produced $\pi^+\pi^-$ final state. A shoulder can also be seen at the square of the kaon mass.

By requiring one of the central particles to have a Cerenkov mass assignment compatible with being a K, p or ambiguous K/p, the Ehrlich mass plot shown in fig.3b is obtained. Three structures

can be seen; these represent the $\pi^+\pi^-$, K^+K^- and $p\bar{p}$ final states. The $\pi^+\pi^-$ peak is due to a misidentification of one of the particles in the Cerenkovs.

4. The $\pi^+\pi^-$ channel

The $\pi^+\pi^-$ channel (≈310,000 events) has been isolated from the other central two-body final states by requiring the Ehrlich mass to be in the range (-0.14 to 0.16 GeV^2). Fig. 4 shows the Feynman x_F distribution for the slow proton, the $\pi^+\pi^-$ system and the fast proton respectively. The majority of the events have the $\pi^+\pi^-$ system concentrated in the region of $|x_F| < 0.2$. Fig. 5 shows the $p_f\pi^+$ and $p_s\pi^+$ distributions which indicate the presence of a Δ^{++} signal due to some contamination from forward and backward diffraction. The $\pi^+\pi^-$ effective mass spectrum is shown in fig.6 after removing the Δ^{++} contamination by requiring $M(p_f\pi^+) > 1.4$ GeV. The distribution shows a suppression of the $\rho(770)$ with respect to the lower energy experiment [5], a sharp drop around the $K\bar{K}$ threshold and an indication of a $f_2(1270)$ signal. A study has been made of the dependence of the $\pi^+\pi^-$ mass spectrum as a function of t ($t = t_1 + t_2$ where t_1 and t_2 are the four momentum transfer from the incident proton to the fast proton and the target to the slow proton respectively). The selected regions are $t < 0.3$ GeV^2 and $t > 0.3$ GeV^2 and are shown in fig. 7. The low t region shows suppressed resonance production but a clear drop at ≈ 1.0 GeV (the so called "S^*") and agrees with the $\pi^+\pi^-$ mass spectrum observed at the ISR [3] in a low t region but at a higher energy ($\sqrt{s} = 62$ GeV). The high t region shows, in addition to the S^*, $\rho(770)$ and $f_2(1270)$ signals. The presence of the $f_2(1270)$ has also been observed at the ISR [4] in a high t region. The $\pi^+\pi^-$ spectrum is particularly interesting since it is through this channel that several models [8] predict that a 0^{++} glueball, with a mass of 1.0 GeV, may decay. A recent analysis [9] of the complex phenomena occurring in this region, especially close to the K^+K^- threshold has indicated the possible presence of such a state.

A simple fit of the $\pi^+\pi^-$ spectrum using the Flatté [10] formalism to describe the S^* has been attempted. Breit-Wigners describing the $\rho(770)$ and $f_2(1270)$ resonances have been included in the fit as well as contamination (in the 0.5 GeV region) due to ω production where the π^0 from the low mo-

mentum ω's has a sufficiently small momentum that it falls inside the momentum balance cuts. The above contamination has been computed by Monte-Carlo simulation and is included as a histogram in the fit.

The expression used for fitting the $\pi^+\pi^-$ mass spectrum is the following

$$dN/dm = \omega(m) + G(m)(B_S(m) + \alpha B_\rho(m) + \beta B_f(m))$$

where $\omega(m)$ represents the ω contamination, $B_\rho(m)$ and $B_f(m)$ represent Breit-Wigner's to describe the $\rho(770)$ and $f_2(1270)$ whose parameters have been fixed to their PDG [11] values. $B_S(m)$ represents the S-wave contribution which has been parametrized as

$$B_S(m) = |1 + \gamma F(m) e^{i\delta}|^2$$

where δ represents a mass independent phase between the S^* resonance and the phase space [12]. The Flatté formalism has been used for the function F(m) having K^+K^- and $K^0\bar{K}^0$ couplings [13].

$$F(m) = \frac{m_0\Gamma_\pi}{m_0^2 - m^2 - im_0(\Gamma_\pi + \Gamma_K)}$$

where

$$\Gamma_\pi = g_\pi\sqrt{((1/4)m^2 - m_\pi^2)}$$

and

$$\Gamma_K = g_K\sqrt{((1/4)m^2 - m_K^2)} + g_K\sqrt{((1/4)m^2 - m_{K^0}^2)}$$

The background has been parameterised as

$$G(m) = a(m - m_{th})^b \exp(-cm - dm^2). \qquad (2)$$

where m is the $\pi^+\pi^-$ mass, m_{th} is the $\pi^+\pi^-$ threshold mass and a,b,c,d are fit parameters. The fit involves 11 parameters and it has been initially performed up to a mass of 1.36 GeV. The parameter, g_K which represents the S^* coupling to $K\bar{K}$ was fixed, while g_π, the coupling to $\pi\pi$, was determined by the fit. Several fits have been performed with different values of g_K. The best χ^2 is obtained when $g_K = 0.075$. It has a fit probability of 17% and is shown in fig. 8. The resulting S^* parameters are $m_0 = 979$ MeV, and $g_\pi = 0.22$.

The S^* parameters have been varied, using as a test the χ^2 computed in the S^* region, which has been defined as the 15 intervals between 0.84 and 1.14 GeV. The χ^2 is 8.4 for $g_K = 0.075$ and increas-

es to 12.3 for $g_K = 0.0$ while the overall fit probability changes from 17% to 3%. The S^* phase has then been set equal to 90^0, i.e. dropping the interference between the S^* function and the background, but fixing g_K to 0.5, which is a relatively high value. The change in χ^2 for this case is significant, increasing to 137.4. Fig. 9 b shows the fit with $g_K = 0.$ (solid curve) and $\delta = 90^0$ with $g_K = 0.5$ (dashed curve).

Thus the main features of the S^* drop observed in the $\pi^+\pi^-$ mass spectrum at the $K\bar{K}$ threshold, is best described by the interference of the resonance with the background even with no coupling to $K\bar{K}$, whereas when interference is excluded a good fit cannot be obtained even with large $K\bar{K}$ coupling.

The fit of the $\pi^+\pi^-$ mass spectrum has then been extended to the region above the $f_2(1270)$, as shown in fig. 9a, where the ω and S-wave contributions have been subtracted. The fit has a bad χ^2 on the high mass side of the $f_2(1270)$. A shoulder in this region has already been observed in other experiments, in particular in the J/ψ radiative decay to $\pi^+\pi^-$ [14] and $\pi^0\pi^0$ [15]. Further analysis is needed in order to understand if this structure is due to an $\varepsilon'(1300)$ contribution which has not been considered in the fit, to interference between the $f'_2(1525)$ and the $f_2(1270)$ or to a new state.

5. The K^+K^- and $K^0_SK^0_S$ channels

Events belonging to the $pp \rightarrow p_f(K^+K^-)p_s$ ($\approx$ 6500 events) final state have been selected by requiring the Ehrlich mass to be in the range (0.16 to 0.56 GeV^2). The mass spectrum is shown in fig.10 and contains several resonance structures; in particular, the $\phi(1020)$ and the $f'_2(1520)$ are clearly seen. A threshold enhancement can also be observed as well as the possible presence of the $f_2(1270)/a_2(1320)$. A structure can also be seen in the 1.7 GeV region. structure which appeared to be resolved into two states.

The $K^0_SK^0_S$ channel has been selected from the sample of events having two reconstructed V^0's and balancing the momentum. In order to remove the background from random $\pi^+\pi^-$ combinations, a decay length of at least 3 cm was required for each of the two V^0's. The $\pi^+\pi^-$ mass spectrum of the

V^0's is shown in fig. 11 and a clear K^0 signal can be seen with little background. Selecting events having the K^0 mass in the range (0.475 to 0.520 GeV) produces the $K^0_S K^0_S$ mass spectrum shown in fig. 12b ($\approx$ 600 events). For comparison, fig. 12a shows the $K^0_S K^0_S$ mass spectrum obtained in the 85 GeV/c experiment ($\approx$ 800 events). The spectra show similar features as the K^+K^- spectrum, a threshold enhancement, some $f_2(1270)/a_2(1320)$, some $f'_2(1525)$ and a structure in the 1.7 GeV region. Since only states with even spins and parity are allowed in the $K^0_S K^0_S$ mass spectrum, it is concluded, from the simultaneous observation of a state in the 1.7 GeV region in both K^+K^- and $K^0_S K^0_S$ systems that it is the $\theta/f_2(1720)$.

In order to measure the $\theta/f_2(1720)$ parameters, a fit has been performed on the data from the 85 and 300 GeV/c runs (fig. 13) in the (1.4 to 2.0 GeV) region by using an exponential background and two non interfering Breit-Wigner's to describe the two resonances. The $f'_2(1520)$ mass was fixed to the PDG value, while the width was fixed to 90 MeV as obtained in recent measurements [16] The fit gives:

$$m(\theta) = 1712 \pm 11 \text{ MeV}$$

$$\Gamma(\theta) = 138 \pm 10 \text{ MeV}$$

with a fit probability of 64%. The same fit has been performed on the K^+K^- spectrum, (see the insert of fig. 10) by fixing the $\theta/f_2(1720)$ width to the one previously determined. The fit gives a mass of

$$m(\theta) = 1706 \pm 15 \text{ MeV}$$

with a fit probability of 41%.

All these measurements of the $\theta/f_2(1720)$ parameters are in agreement with previous determinations in J/ψ decays [14]. This observation reinforces the possibility of the $\theta/f_2(1720)$ being a gluonium state since it has only been seen in reactions which are supposed to be gluon rich and is not produced by incident K^- reactions [16] and $\gamma\gamma$ collisions [17].

The $p\bar{p}$ effective mass is shown in fig. 14 and does not show resonance production.

6. The $K^0_S K^{\pm}\pi^{\mp}$ channel

After selecting events having four outgoing tracks plus a V^0 the "4C" candidates were isolated by applying cuts to the components of missing momentum. Fig.15 shows the $\pi^+\pi^-$ mass distribution for the V^0's; a good K^0 signal is seen with σ = 7 MeV. The K^0 is selected by requiring $0.475 < m(\pi^+\pi^-) < 0.52$ GeV.

The reaction

$$pp \rightarrow p_f(K^0_S K^{\pm}\pi^{\mp})p_s$$

was selected from this sample by using energy conservation. A cut of $|\Delta| \leq 1.6\ (GeV)^2$ was used, where

$$\Delta = MM^2(pp) - M^2(K^0_S K^{\pm}\pi^{\mp}) .$$

In addition Cerenkov compatibility was required.

Fig.16 shows the $K^0_S K^{\pm}\pi^{\mp}$ effective mass spectrum (4606 events) where the events that have an ambiguous $K^{\pm}\pi^{\mp}$ mass assignment are plotted twice (28.8 % of the events). Fig.17 shows the $K^0_S K^{\pm}\pi^{\mp}$ mass spectrum where one of the particle is required to be identified as a K or K/p by the Cerenkov system (939 events).

A fit to the spectrum, without taking the resolution into account, using two Breit-Wigners and a background of the form $a(m-m_{th})^b exp(-cm-dm^2)$ (where m is the $K^0_S K^{\pm}\pi^{\mp}$ mass, m_{th} is the $K^0_S K^{\pm}\pi^{\mp}$ threshold mass and a,b,c,d are fit parameters), yields masses and widths of

$$M_1 = 1280 \pm 2 \text{ MeV} \quad \Gamma_1 = 17 \pm 4 \text{ MeV}$$

$$M_2 = 1431 \pm 2 \text{ MeV} \quad \Gamma_2 = 45 \pm 4 \text{ MeV}$$

6.1 Preliminary Spin−Parity Analysis of the $K^0_S K^{\pm}\pi^{\mp}$ System

6.1.1 The $f_1(1285)$ Region

A preliminary Dalitz plot analysis of the $K^0_S K^{\pm}\pi^{\mp}$ mass spectrum has been performed by using a standard isobar model [18]. Fits to the $f_1(1285)$ region (1.25−1.32 GeV, 214 events) have been performed using amplitudes describing the 0^{-+}, 1^{++}, and 2^{-+} states decaying through $\delta\pi$, where the δ has been described in terms of the Flatté formalism [19]. The fits show that two solutions are possible

a. $\approx$100 % 0^{-+} wave with zero background. The fit has a Log Likelihood of 40.

b. 70$\pm$5 % 1^{++} wave with 30% phase space background. The fit has a Log Likelihood of 44.

These waves were used as input to a Monte Carlo program in order to generate a Dalitz plot. This has been used in a Least Square test with the real data. The 0^{-+} wave has a χ^2/NDF of 64/37 while for the 1^{++} wave the χ^2/NDF is 47/37. Hence the 1^{++} wave gives the best fit to the data which is consistent with the result obtained at 85 GeV/c.

6.1.2 The $f_1(1420)$ Region

Fig.18 shows the Dalitz plot in the $f_1(1420)$ region defined as $1.37 \leq M(K^0_S K^{\pm}\pi^{\mp}) \leq 1.49$ GeV with $K\pi$ and $K\bar{K}$ projections. There are 753 events in the plot, well defined K^* bands can be seen but there is no enhancement near threshold in the $K\bar{K}$ spectrum.

The $f_1(1420)$ region has been fitted in 40 MeV slices from 1.33 to 1.69 GeV so that the background can also be studied. Full interference between waves having the same spin-parity has been allowed. Interference was also allowed between the 1^{++} and 1^{+-} $K^*\bar{K}$ waves.

The fit shows that the $1^{++}(K^*\bar{K})$ is the dominant wave. The addition of any 0^{-+} or any other waves does not increase the Log Likelihood. A fit including 0^{-+} and 1^{++} S waves is shown in fig.19. If the $f_1(1420)$ region is defined as $1.37 \leq M(K^0_S K^{\pm}\pi^{\mp}) \leq 1.49$ GeV then the percentage of each wave present is

$$0^{-+} \quad 4.0 \pm 2\ \%$$

$$1^{++}\ S \quad 50 \pm 3\%$$

Therefore it is concluded that the 0^{-+} waves are consistent with zero and only the 1^{++} wave is needed. A fit with 1^{++} and phase space only gives

$$1^{++}\ S \quad 53\pm4\ \%$$

with 47 % background.

7. The $\pi^+\pi^-\pi^+\pi^-$ channel.

After selecting events having six outgoing tracks that balance momentum, the events are required to have a Cerenkov mass assignment compatible with being a π and the Δ function defined by

$$\Delta = MM^2(pp) - M^2(\pi^+\pi^-\pi^+\pi^-)$$

is used to select out the "4C" candidates.

There is $\approx$ 5 % Δ^{++} production in the effective mass spectrum of the $p_f\pi^+$ but no evidence for Δ^0 production in the $p_f\pi^-$ mass spectrum. A cut is used of $M(p_f\pi^+) < 1.4$ GeV to remove the Δ^{++} production.

Fig.20a shows the 4π effective mass spectrum ($\approx$50000 events); the $f_1(1285)$ can clearly be seen. There is also clear evidence for a structure around 1.45 GeV.

A fit has been performed to this spectrum using two relativistic Breit-Wigners, in the 1.28 and 1.45 GeV regions, with a background of the form $a(m-m_{th})^b\exp(-cm-dm^2)$ (where m is the $\pi^+\pi^-\pi^+\pi^-$ mass, m_{th} is the $\pi^+\pi^-\pi^+\pi^-$ threshold mass and a,b,c,d are fit parameters), and two histograms that have been generated from real data to simulate the η' and $f_1(1285)$ reflections from the $\eta\pi^+\pi^-$ channel. The fit has a χ^2/NDF of 244/141 (not shown). The major contribution to the χ^2 comes from a broad enhancement at 1.9 GeV. Introducing a third Breit-Wigner in the region of 1.9 GeV produces a fit, shown in fig.20b, with a χ^2/NDF of 121/138 corresponding to a fit probability of 85 %.

The fit parameterisation has been changed in several ways in order to investigate the effect on the parameters of the Breit-Wigner describing the 1.45 GeV region but no change outside the errors is observed. The parameterisation of the Breit-Wigners used in the fit shown in fig.20b is summarised in table 1.

In conclusion a structure is observed in the $f_1(1420)/\eta(1440)$ region that has a mass somewhat higher than the $f_1(1420)$ observed in the $K^0_SK^\pm\pi^\mp$ channel which leaves open the interpretation of this state.

Table 1: Parameters of resonances in the fit to the 4π spectrum

With Statistical errors coming from the fit

Mass 1	1285	±	1	MeV
Γ 1	30	±	3	MeV
Mass 2	1454	±	5	MeV
Γ 2	88	±	12	MeV
Mass 3	1923	±	15	MeV
Γ 3	377	±	54	MeV

8. Discussion and Conclusions

This paper reports on a preliminary analysis of data taken using a double exchange reaction trigger at an incident beam momenta of 300 GeV/c in which exclusive channels have been isolated. The results to date can be summarised as follows

a. The $\pi^+\pi^-$ mass spectrum shows little $\rho(770)$ production with respect to the 85 GeV/c run; some $f_2(1270)$ is observed, especially in the high t region. A drop is observed in the S^* region which has been fitted by means of a coupled channel Breit-Wigner interfering with the background. This gives $g_K = 0.075$, $g_\pi = 0.22$ and a mass of 979 MeV. The main features of the S^* drop observed in the $\pi^+\pi^-$ mass spectrum at the $K\bar{K}$ threshold, is best described by the interference of the resonance with the background even with no coupling to $K\bar{K}$, whereas when interference is excluded a good fit cannot be obtained even with large $K\bar{K}$ coupling.

b. The K^+K^- and the $K^0_S K^0_S$ mass spectra show consistent resonance production. A threshold enhancement is seen in both spectra, and the ϕ is seen decaying to K^+K^-. The high mass region shows evidence for the $f'_2(1520)$ and a state which is interpreted as the $\theta/f_2(1720)$ at a

mass of 1712±11 MeV with a width of 138±10 MeV ($K^0_S K^0_S$) and a mass of 1706±15 MeV (K^+K^-). This new observation in hadronic production reinforces the possibility that the $\theta/f_2(1720)$ is a gluonium state since it has only been seen in reactions which are supposed to be gluon rich and is not produced by incident K^- reactions [16] and $\gamma\gamma$ collisions [17].

c. Clear $f_1(1285)$ and $f_1(1420)$ signals are seen in the $K\bar{K}\pi$ channel. A preliminary spin parity analysis shows that both are consistent with being 1^{++} states. The $f_1(1420)$ is found to decay only to $K^*\bar{K}$ and no 0^{-+} wave is required to describe the data.

d. The $\pi^+\pi^-\pi^+\pi^-$ spectrum shows a clear $f_1(1285)$ as well as an enhancement at 1454 ± 5 MeV with a width of 88 ± 12 MeV. There appears also to be some evidence for a structure in the 1.9 GeV region.

References

[1] M.Benayoun et al., Phys. Lett., **B198** (1987) 281.

[2] G.Eigen Proceedings of the Int. School of Physics with low energy antiprotons-2nd course: Spectroscopy of light and heavy quarks, Erice 23-31 May 1987.

[3] T. Akesson et al., Nucl. Phys. **B264** (1986) 154.

[4] A. Breakstone at al., Z. Phys. **C27** (1985) 205.

[5] G. Vassiliadis et al., Proceedings of the International Conference on Hadron Spectroscopy, University of Maryland, 20 – 22 April, 1985.

[6] D.M.Chew and G.F.Chew, Phys. Lett. **53B** (1974) 191.

[7] R.Ehrlich et al., Phys. Rev. Lett. **20** (1968) 686.

[8] C.E. Carlson et al., Phys. Rev. **D30** (1984) 1594.

[9] K.L. Au et al., Phys. Rev. **D35** (1987) 1633.

[10] S.M. Flatté et al., Phys. Lett. **38B** (1972) 232.

[11] Particle Data Group, Phys. Lett., **170B** (1986).

[12] N. Isgur Private communication

[13] M. Buttram et al., Phys. Rev. **D13** (1976) 1153.

[14] R.M. Baltrusaitis et al., Phys. Rev. **D35** (1987) 2077.

[15] C. Edwards et al., Phys. Rev. **D25** (1982) 3065.

[16] D. Aston et al., Nucl. Phys. **B301** (1988) 525.

[17] H. Aihara et al., Phys. Rev. Lett. **57** (1986) 404.

[18] Ch.Zemach, Phys. Rev. **133B** (1964) 1201.
C.Dionisi et al., Nucl. Phys. **B169** (1980) 1.

[19] S.M.Flatté, Phys. Lett. **63B** (1976) 224.

9. Figures

Fig. 1 Layout of the Ω spectrometer in experiment WA76

Fig. 2 a) Missing transverse momentum distribution for the four prong events.

b) Missing longitudinal momentum distribution for the four prong events after a cut on the missing P_T

Fig. 3 a) Ehrlich mass distribution for all the four prong events

b) Ehrlich mass distribution for the four prong events were one of the central particles is identified by the Cerenkovs as being a K, p or K/p.

Fig. 4 Feynman x distribution for the $p_f(\pi^+\pi^-)p_s$ system.

Fig. 5 a) $M(p_f\pi^+)$ distribution in $p_f(\pi^+\pi^-\pi^+\pi^-)p_s$.

b) $M(p_f\pi^-)$ distribution in $p_f(\pi^+\pi^-\pi^+\pi^-)p_s$.

Fig. 6 The $\pi^+\pi^-$ effective mass spectrum

Fig. 7 The $\pi^+\pi^-$ effective mass spectrum

a) $t < 0.3$ GeV^2 b) $t > 0.3$ GeV^2

Fig. 8 The $\pi^+\pi^-$ effective mass spectrum with fit. The lower histogram represents the resulting $\rho(770)$ and $f_2(1270)$ contributions

Fig. 9 The $\pi^+\pi^-$ effective mass spectrum with fit

a) After background subtraction.

b) Effect of changing the parameters of the fit (see text).

Fig. 10 The K^+K^- effective mass spectrum with fit

Fig. 11 Effective mass distribution of the $\pi^+\pi^-$ pairs.

Fig. 12 $K^0_S K^0_S$ Effective mass spectrum from a) the 85 GeV/c run and b) the 300 GeV/c run

Fig. 13 $K^0_S K^0_S$ effective mass from the 85 and 300 GeV/c runs. The line is the result of the fit described in the text.

Fig. 14 $p\bar{p}$ effective mass spectrum

Fig. 15 Effective mass distribution of the $\pi^+\pi^-$ pairs coming from V^0's.

Fig. 16 $K^0_S K^{\pm}\pi^{\mp}$ mass distribution with fit.

Fig. 17 $K^0_S K^{\pm}\pi^{\mp}$ mass distribution requiring a K or K/p identified, with fit .

Fig. 18 Dalitz plot with projections for the mass region $1.37 - 1.49$ GeV

Fig. 19 Result of the Dalitz plot analysis for the 1^{++} S, 0^{-+} and Phase space.

Fig. 20 a) The 4π effective mass spectrum

b) The 4π effective mass spectrum with fit using 3 Breit-Wigners.

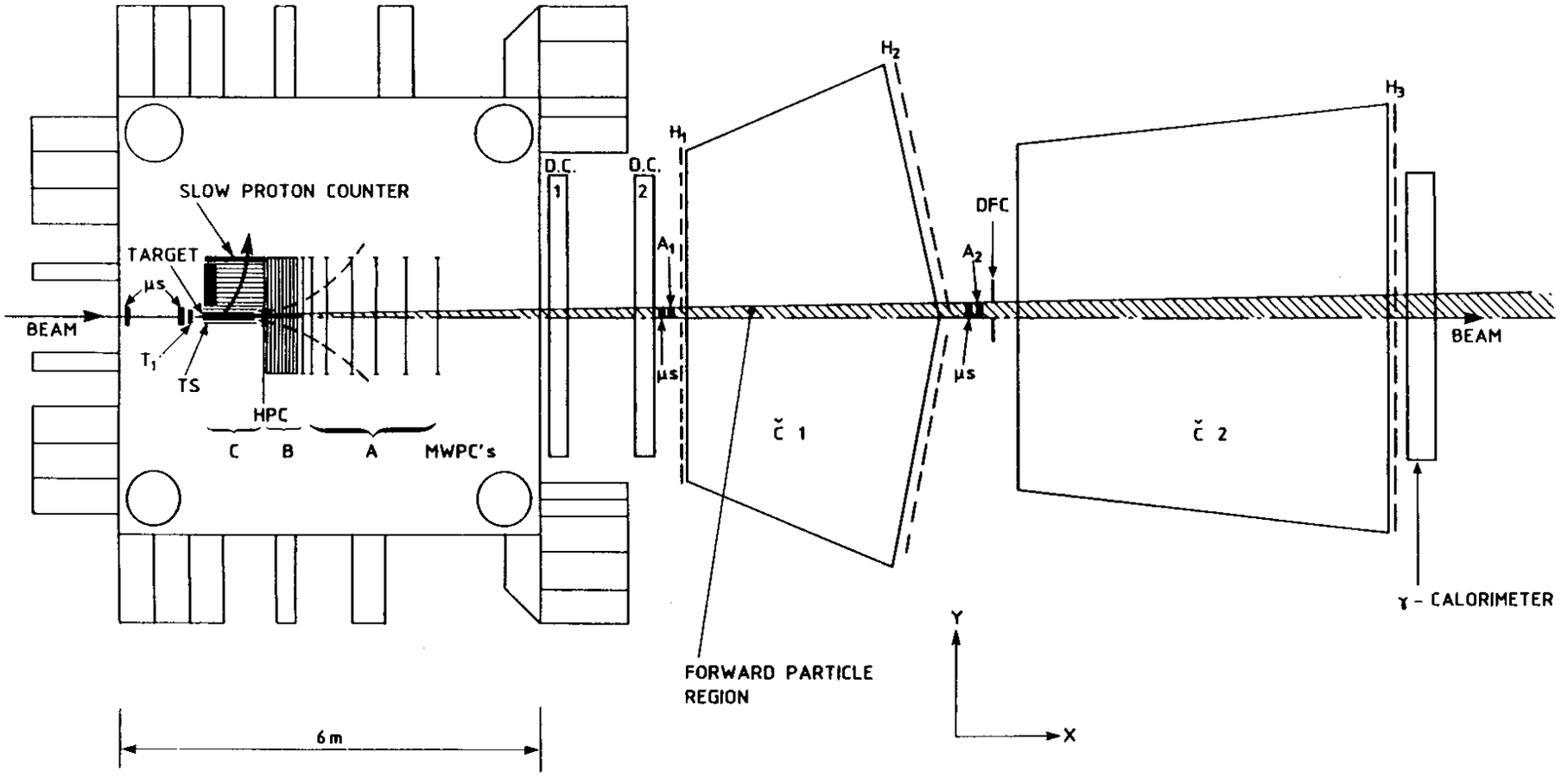
SLOW PROTON COUNTER
TARGET
μs
BEAM
T1
TS
HPC
C
B
A
MWPC's
D.C.
1
D.C.
2
H1
H2
H3
A1
A2
DFC
μs
μs
Č 1
Č 2
BEAM
γ - CALORIMETER
FORWARD PARTICLE
REGION
Y
X
6 m

Fig.1

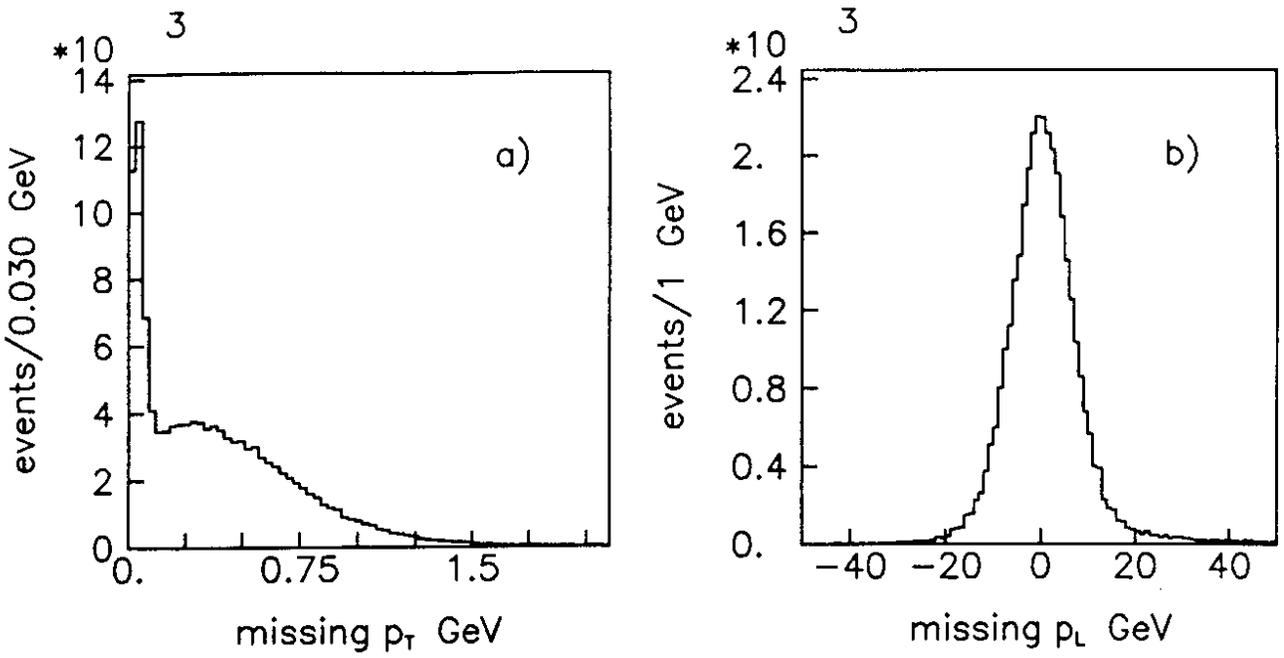
*10 3
events/0.030 GeV
a)
missing p_T GeV
*10 3
events/1 GeV
b)
missing p_L GeV

Fig.2

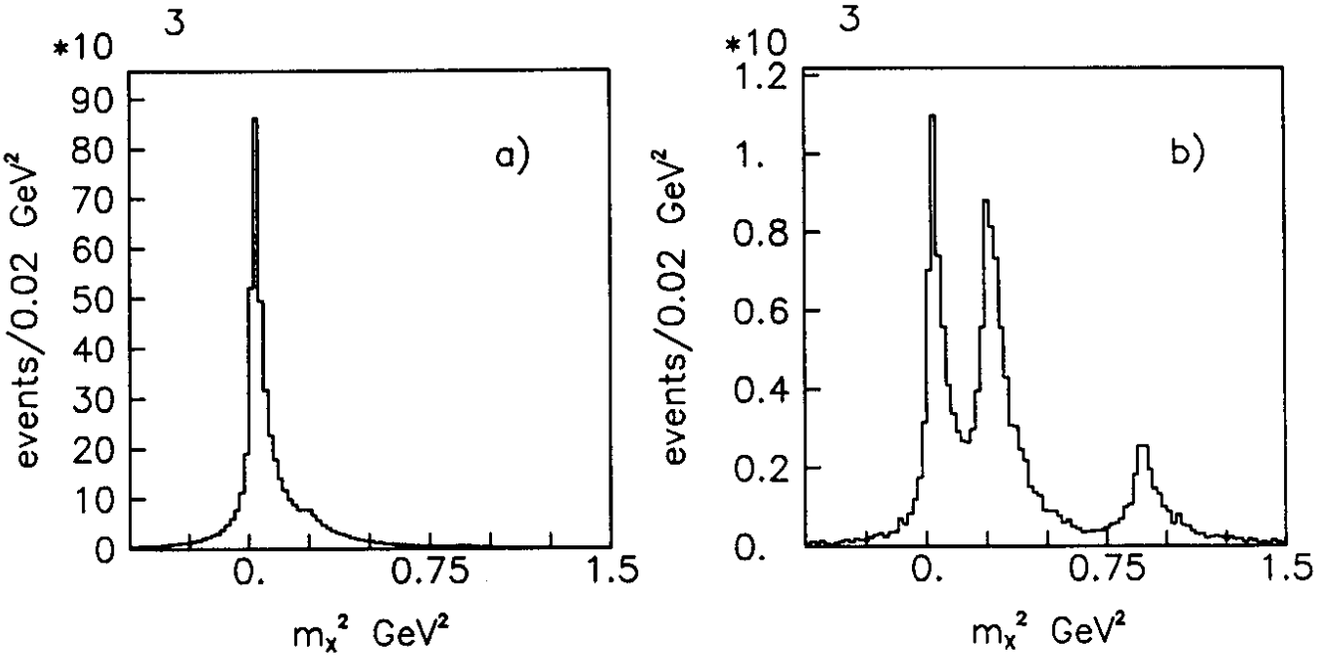
*10 3
events/0.02 GeV²
a)
m_x^2 GeV²
*10 3
events/0.02 GeV²
b)
m_x^2 GeV²

Fig.3

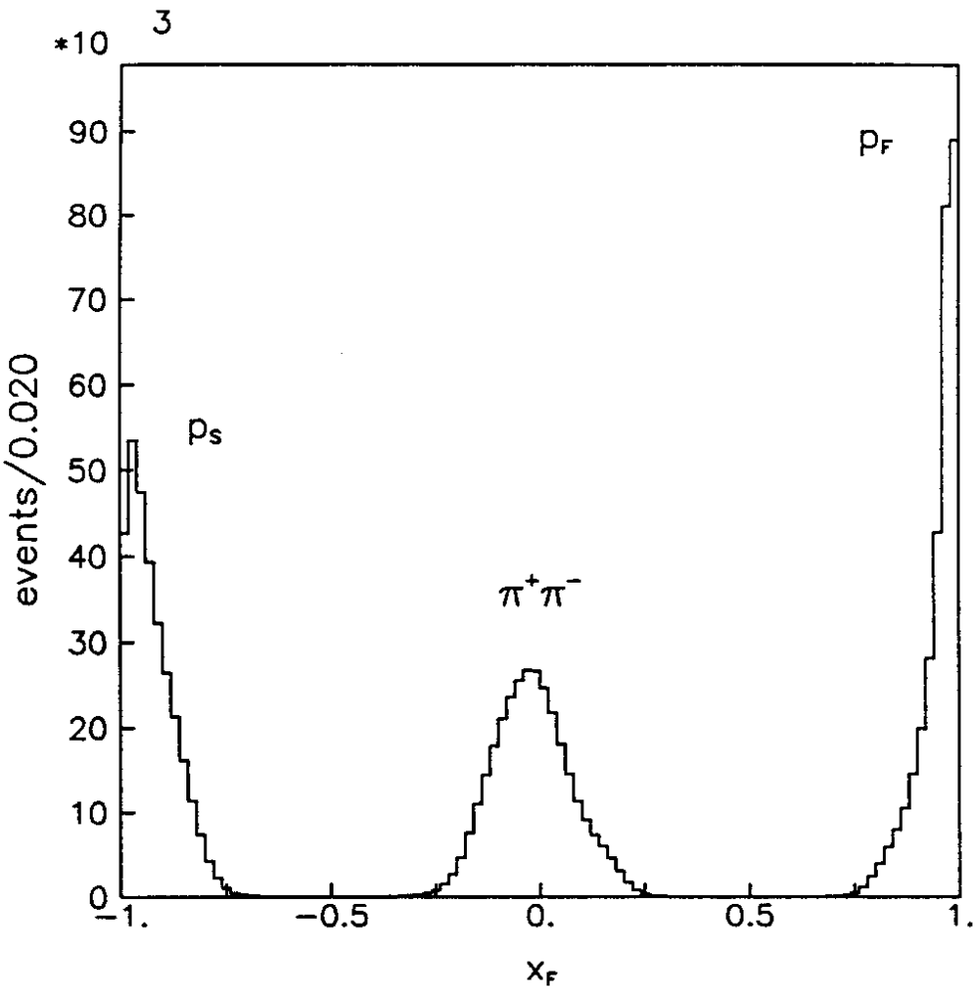
*10 3
events/0.020
p_F
p_s
$\pi^+\pi^-$
x_F

Fig.4

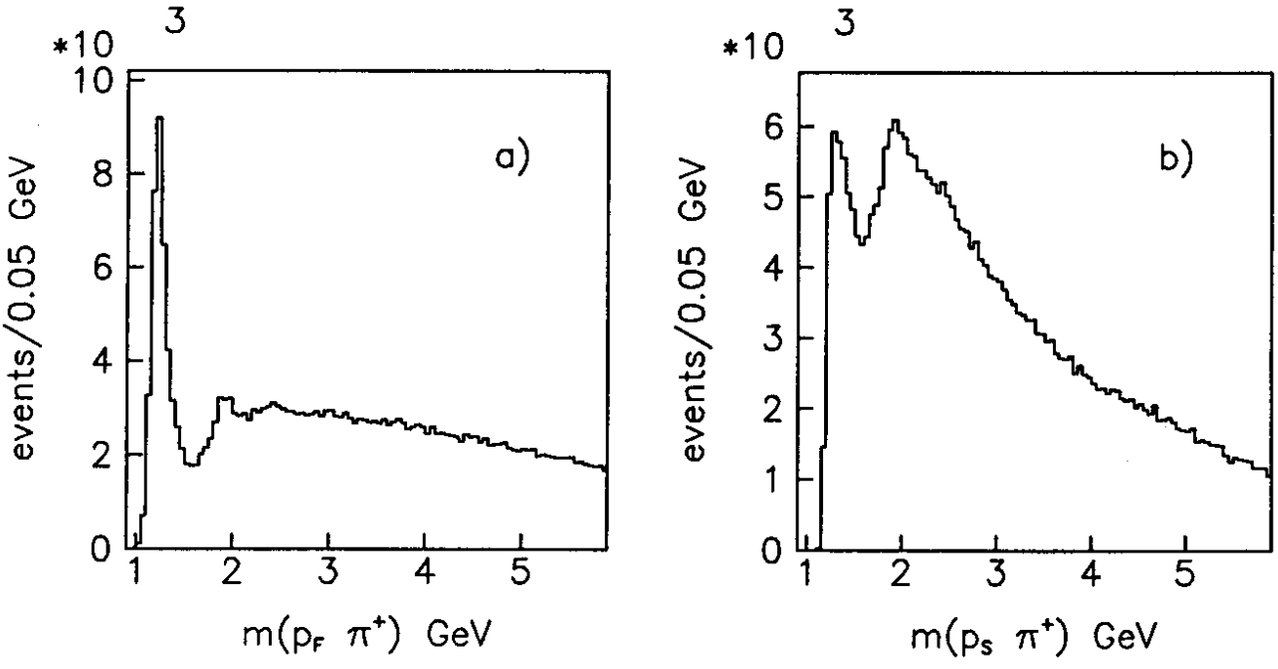
*10 3
events/0.05 GeV
a)
$m(p_F\ \pi^+)$ GeV
*10 3
events/0.05 GeV
b)
$m(p_s\ \pi^+)$ GeV

Fig.5

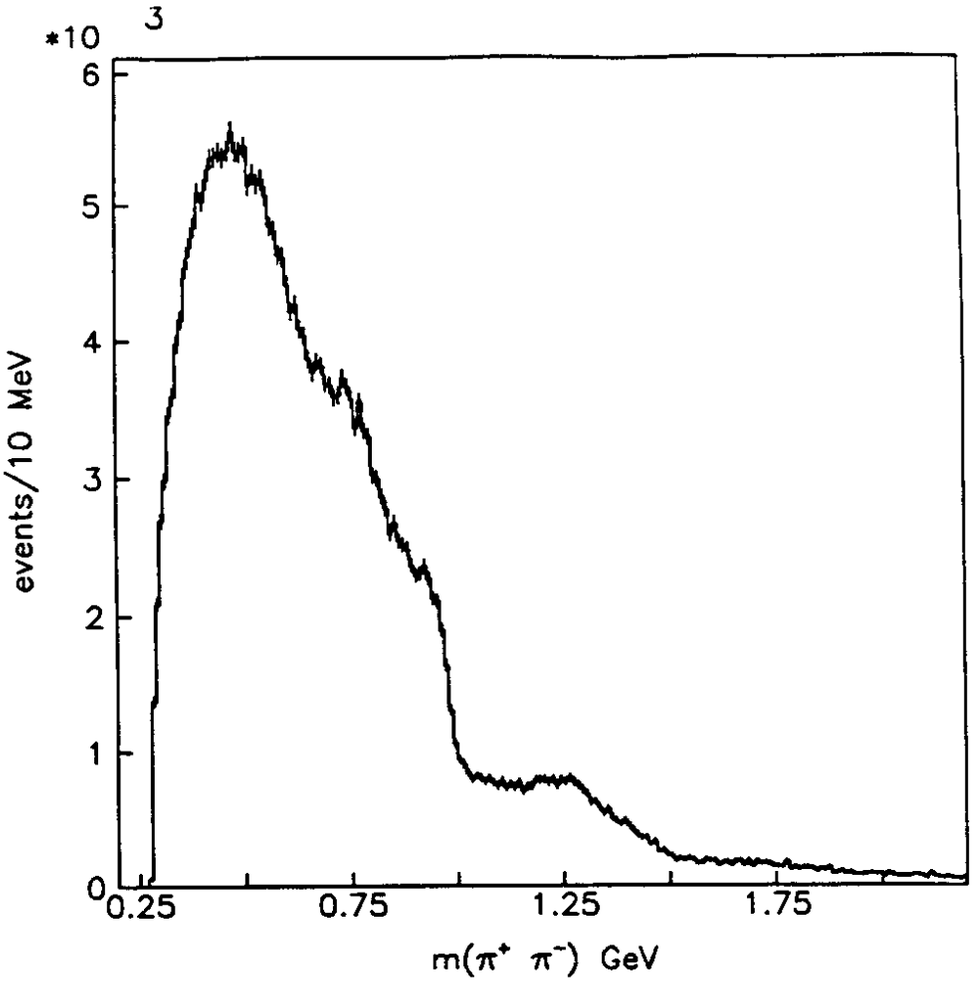
*10 3
events/10 MeV
m(π⁺ π⁻) GeV

Fig.6

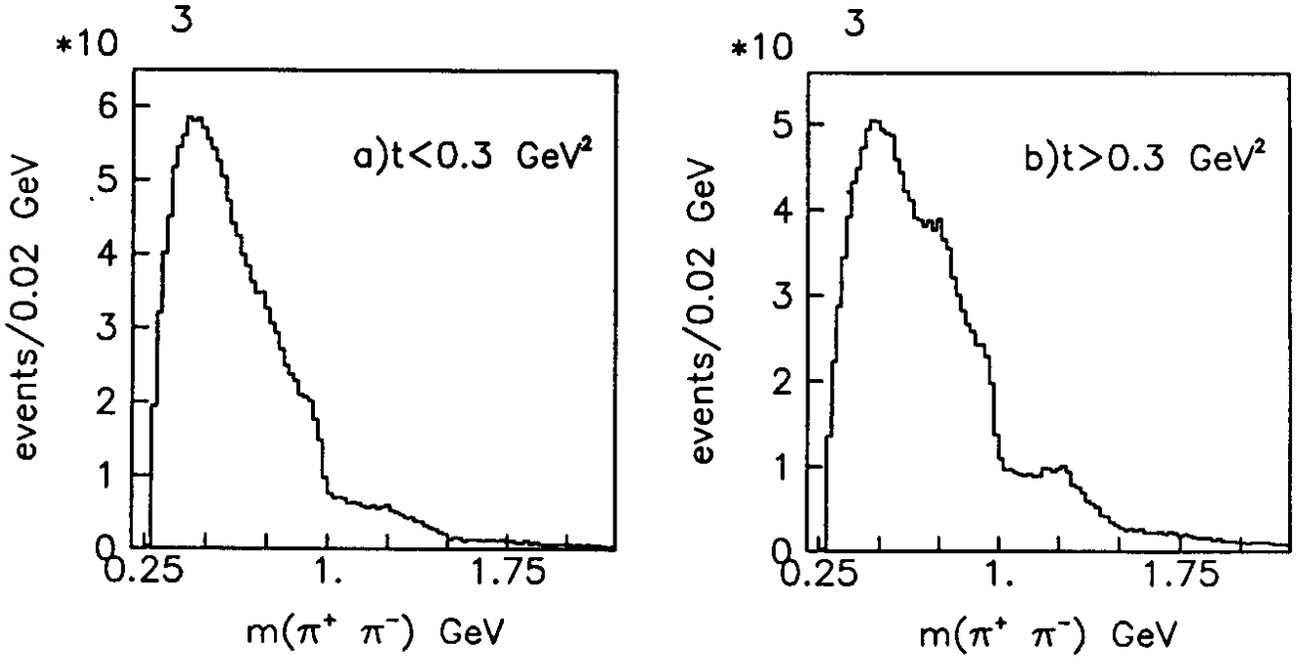
*10 3
a)t<0.3 GeV²
events/0.02 GeV
m(π⁺ π⁻) GeV
*10 3
b)t>0.3 GeV²
events/0.02 GeV
m(π⁺ π⁻) GeV

Fig.7

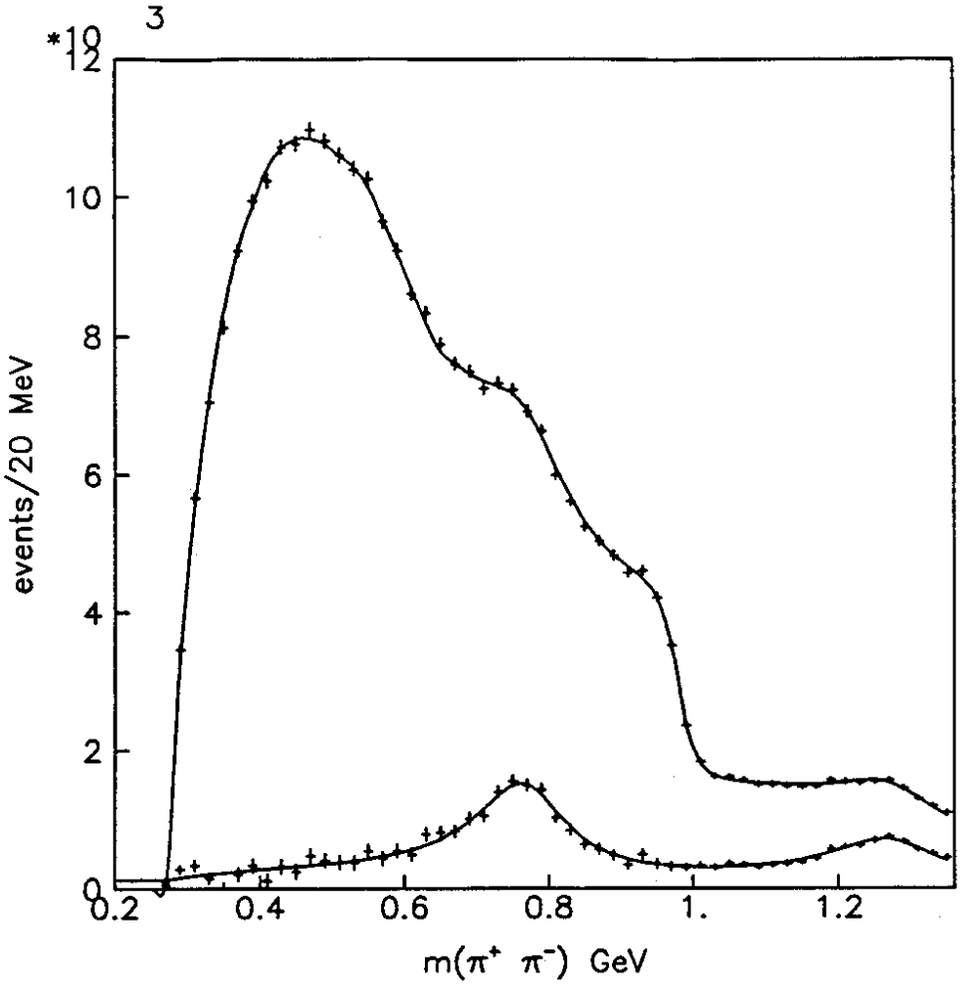
*10 3
12
10
8
6
4
2
0
events/20 MeV
0.2
0.4
0.6
0.8
1.
1.2
m(π⁺ π⁻) GeV

Fig.8

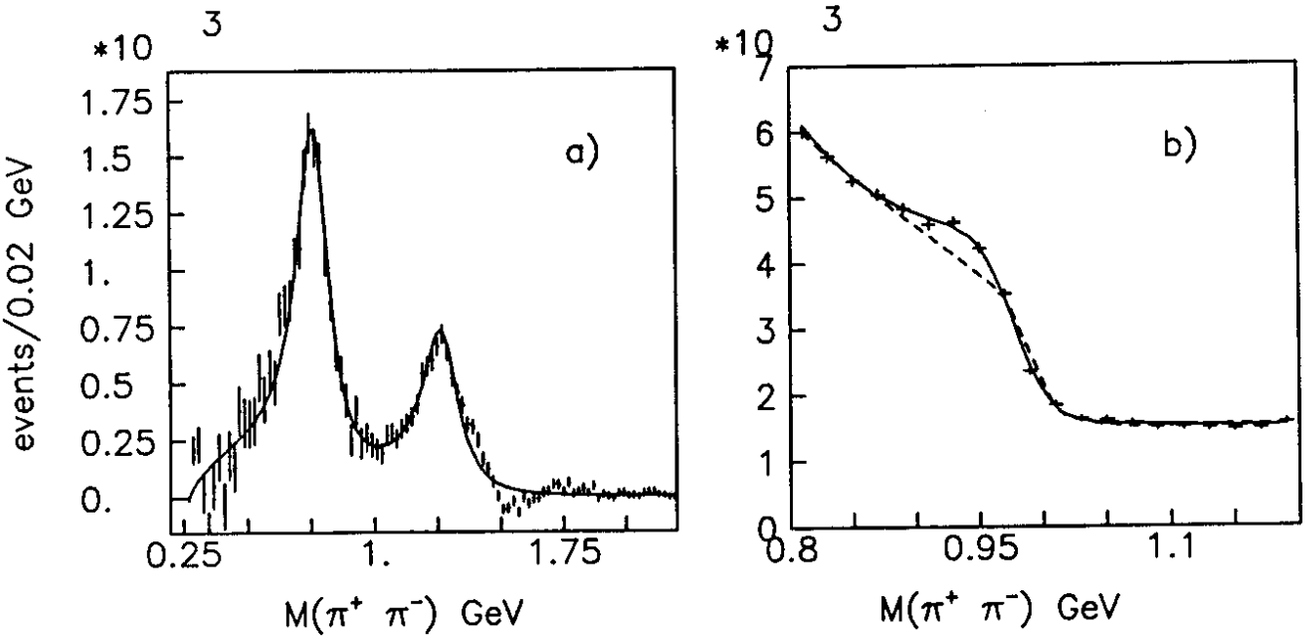
*10 3
1.75
1.5
1.25
1.
0.75
0.5
0.25
0.
events/0.02 GeV
a)
0.25
1.
1.75
M(π⁺ π⁻) GeV
*10 3
7
6
5
4
3
2
1
0
b)
0.8
0.95
1.1
M(π⁺ π⁻) GeV

Fig.9

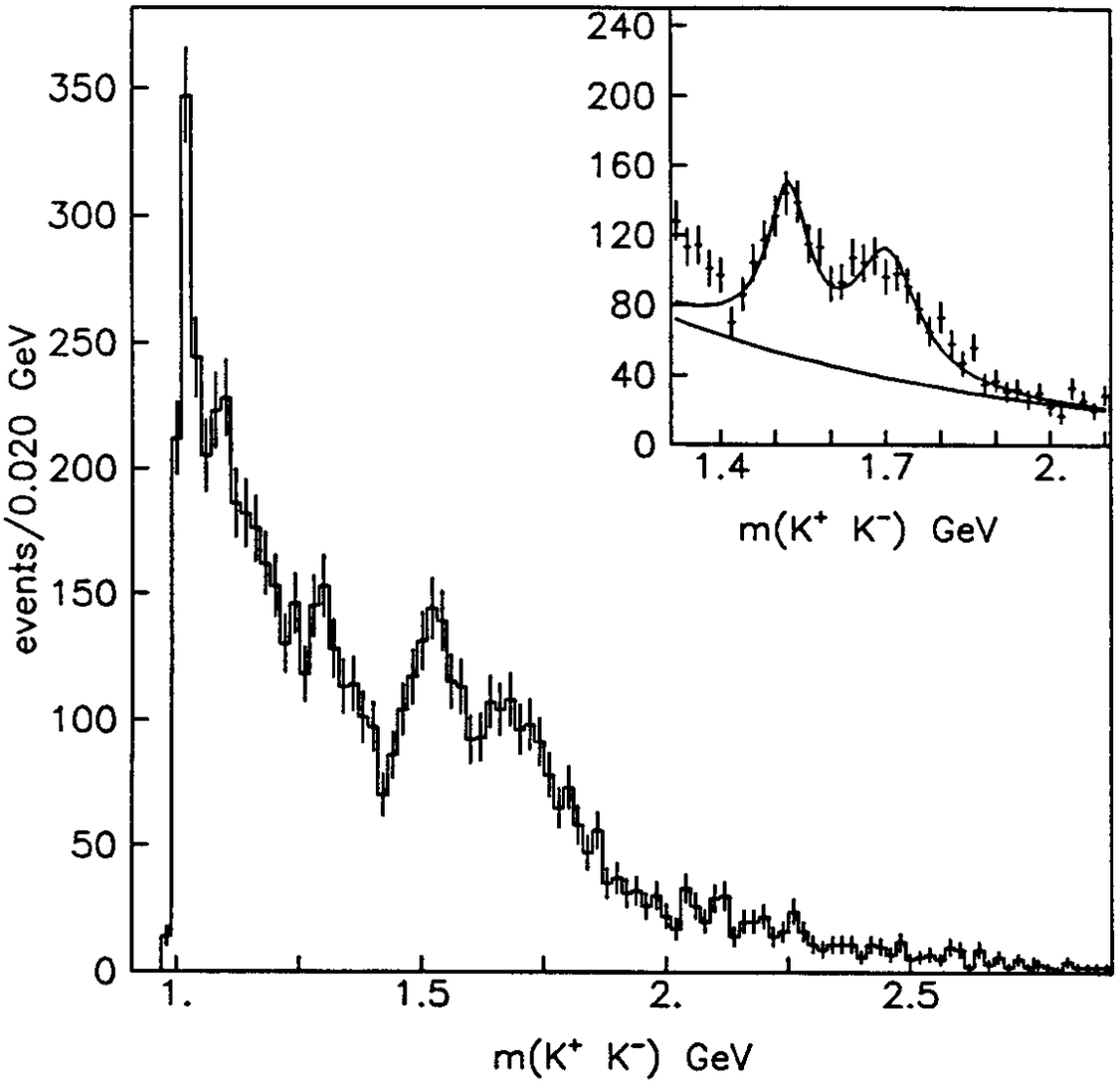
events/0.020 GeV
350
300
250
200
150
100
50
0
1.
1.5
2.
2.5
m(K⁺ K⁻) GeV
240
200
160
120
80
40
0
1.4
1.7
2.
m(K⁺ K⁻) GeV

Fig.10

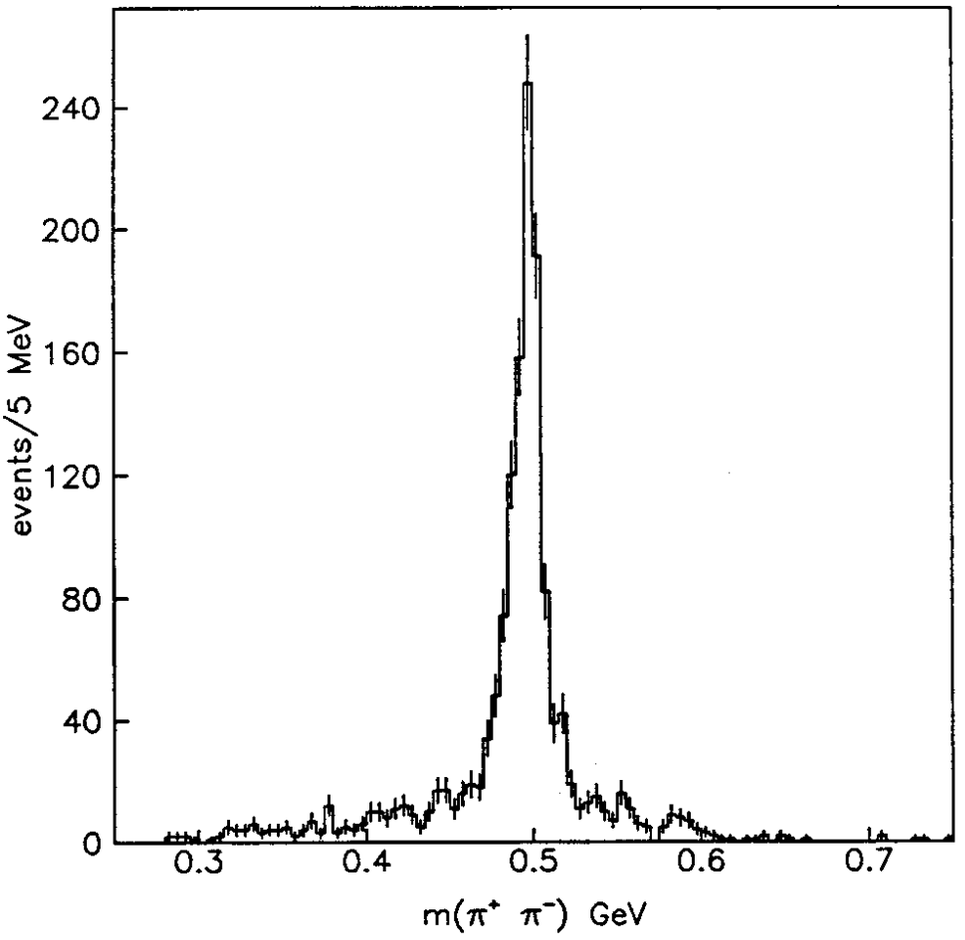
events/5 MeV
240
200
160
120
80
40
0
0.3
0.4
0.5
0.6
0.7
m(π⁺ π⁻) GeV

Fig.11

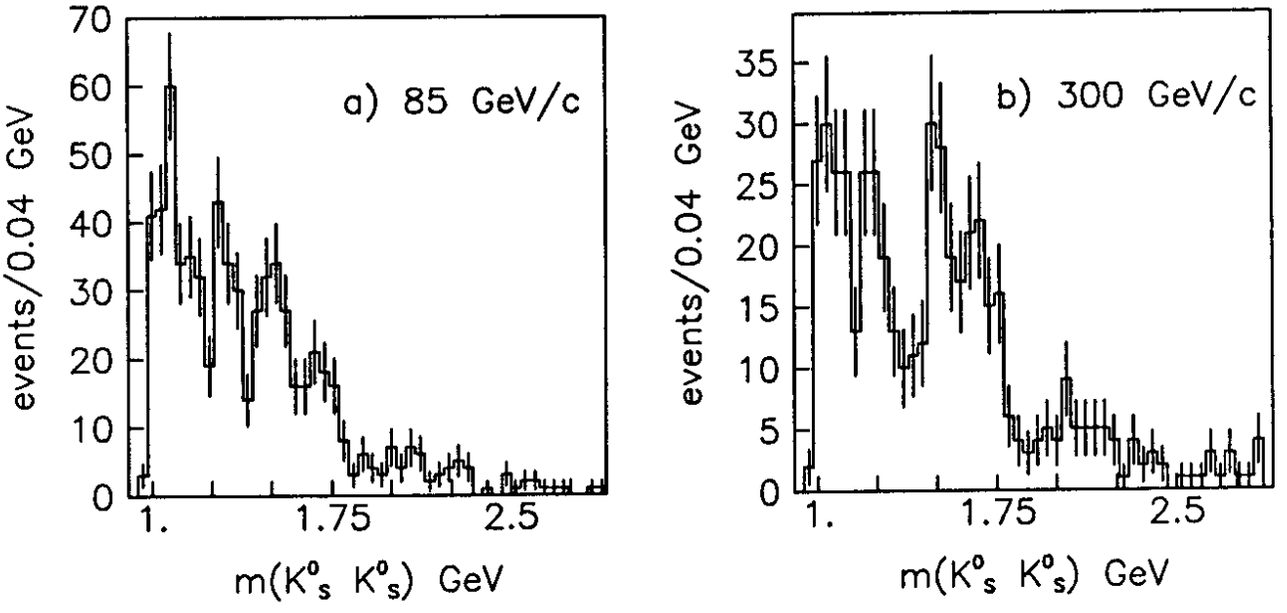
events/0.04 GeV
a) 85 GeV/c
70
60
50
40
30
20
10
0
1.
1.75
2.5
m(K⁰s K⁰s) GeV
events/0.04 GeV
b) 300 GeV/c
35
30
25
20
15
10
5
0
1.
1.75
2.5
m(K⁰s K⁰s) GeV

Fig.12

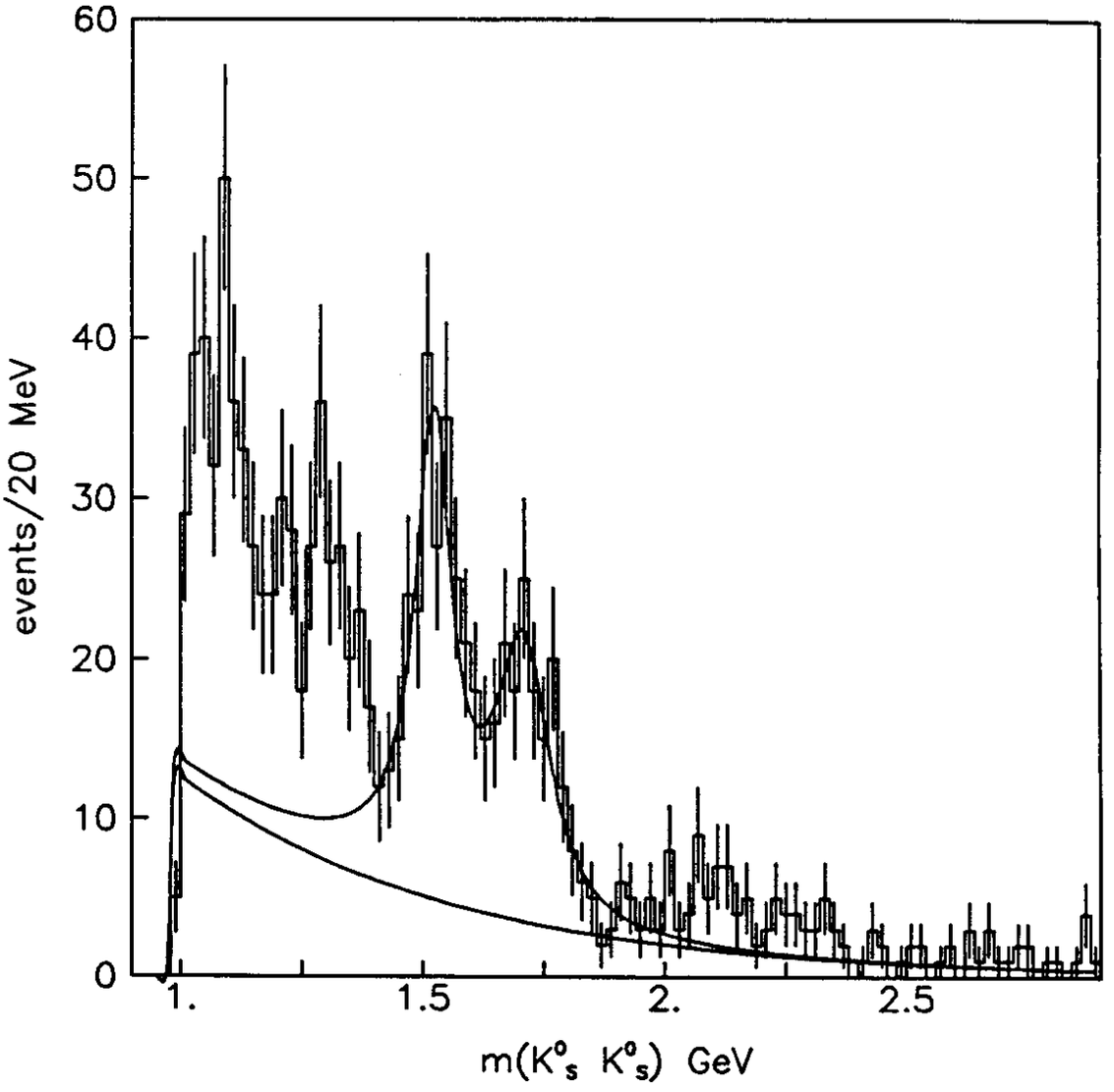

Fig.13

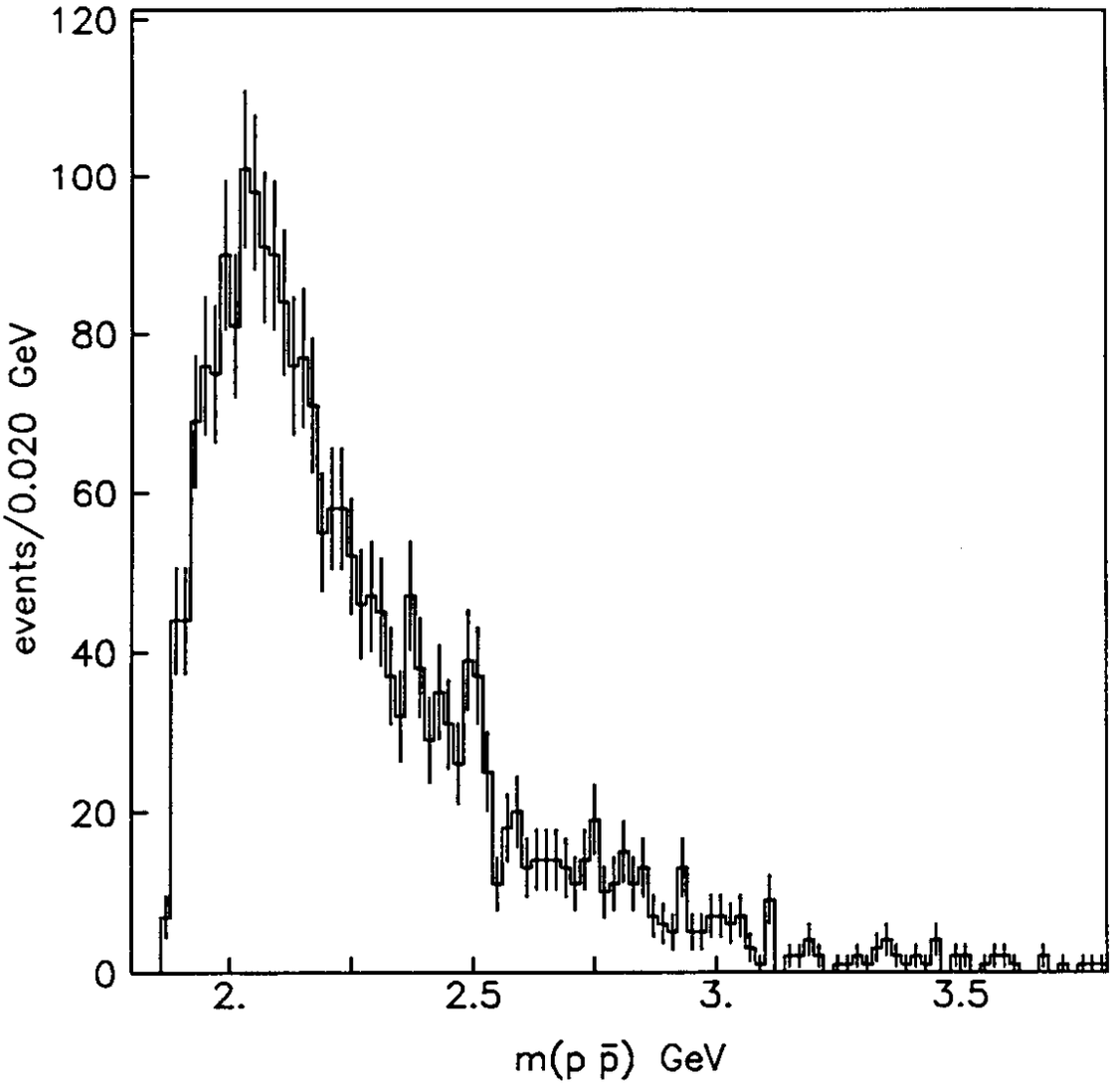

Fig.14

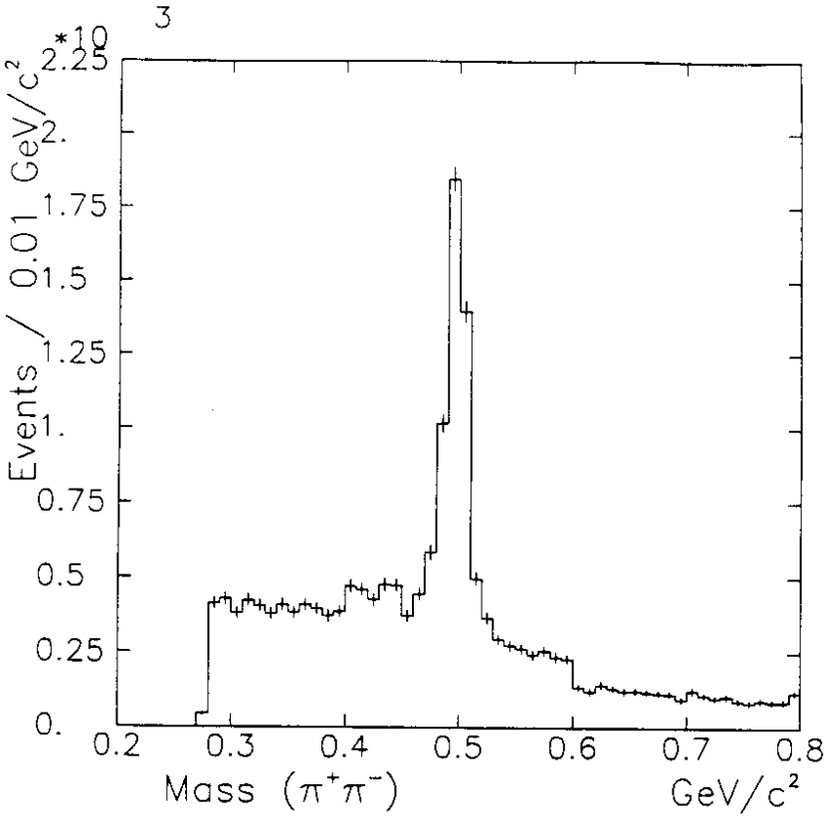
*10 3
Events / 0.01 GeV/c²
2.25
2.
1.75
1.5
1.25
1.
0.75
0.5
0.25
0.
0.2
0.3
0.4
0.5
0.6
0.7
0.8
Mass (π⁺π⁻)
GeV/c²

Fig.15

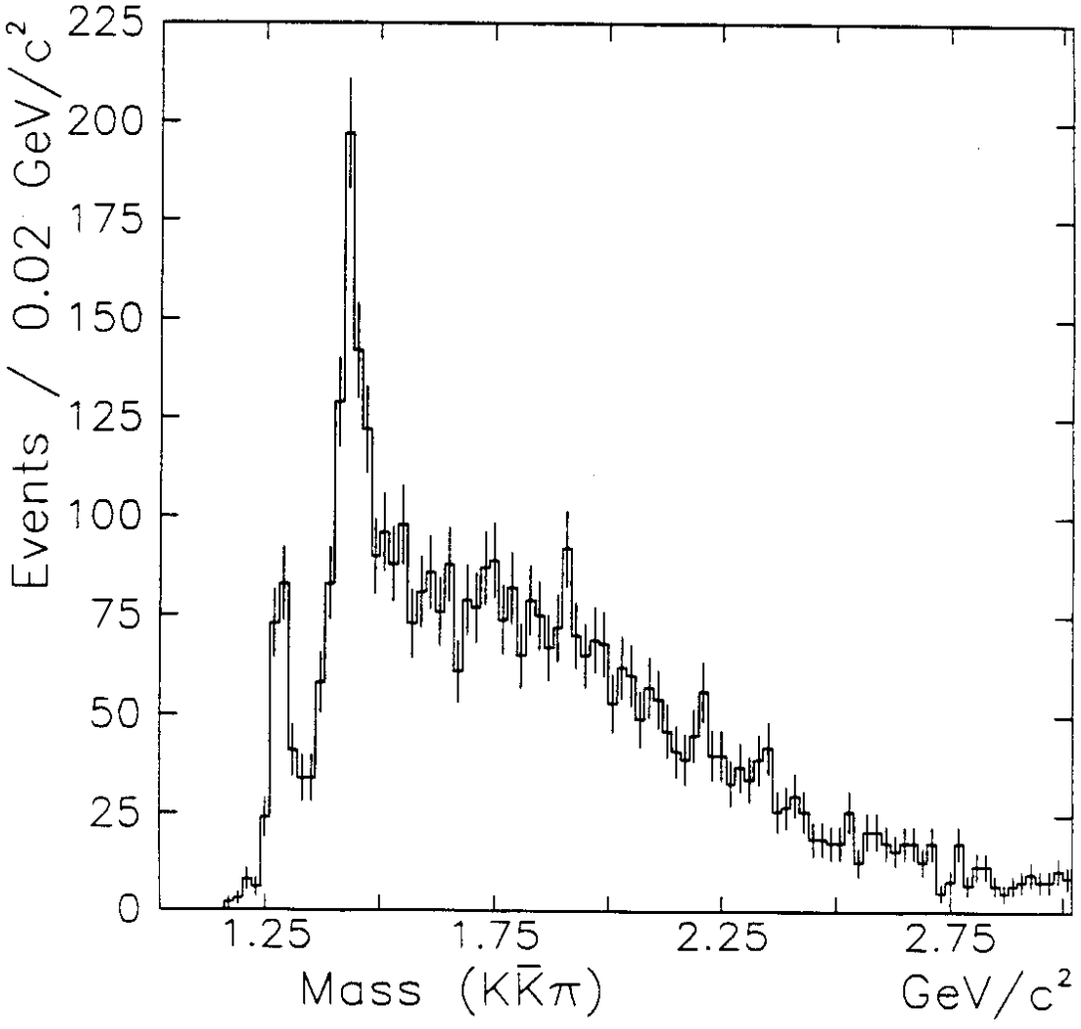
Events / 0.02 GeV/c²
225
200
175
150
125
100
75
50
25
0
1.25
1.75
2.25
2.75
Mass (KK̄π)
GeV/c²

Fig.16

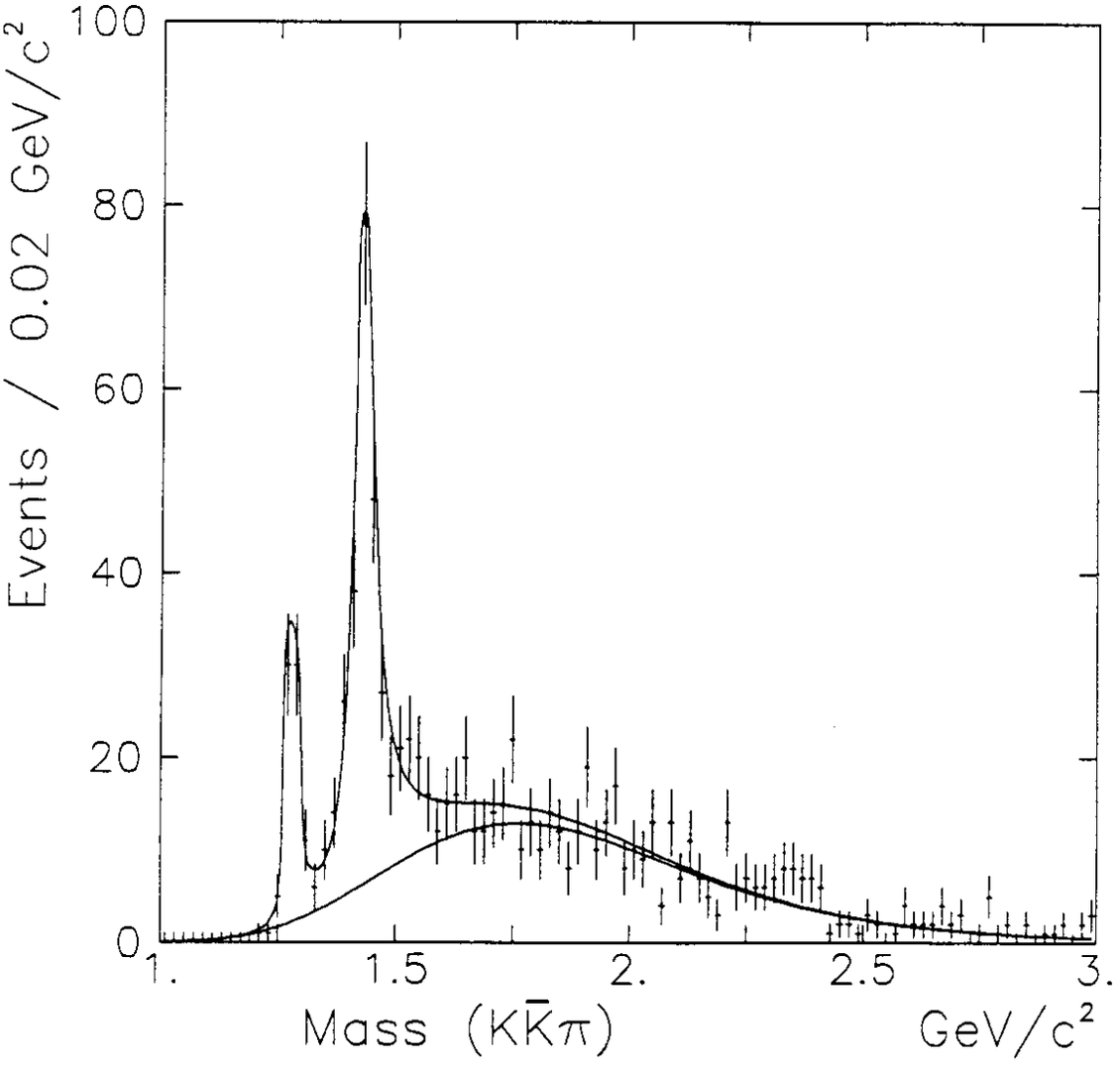

Fig.17

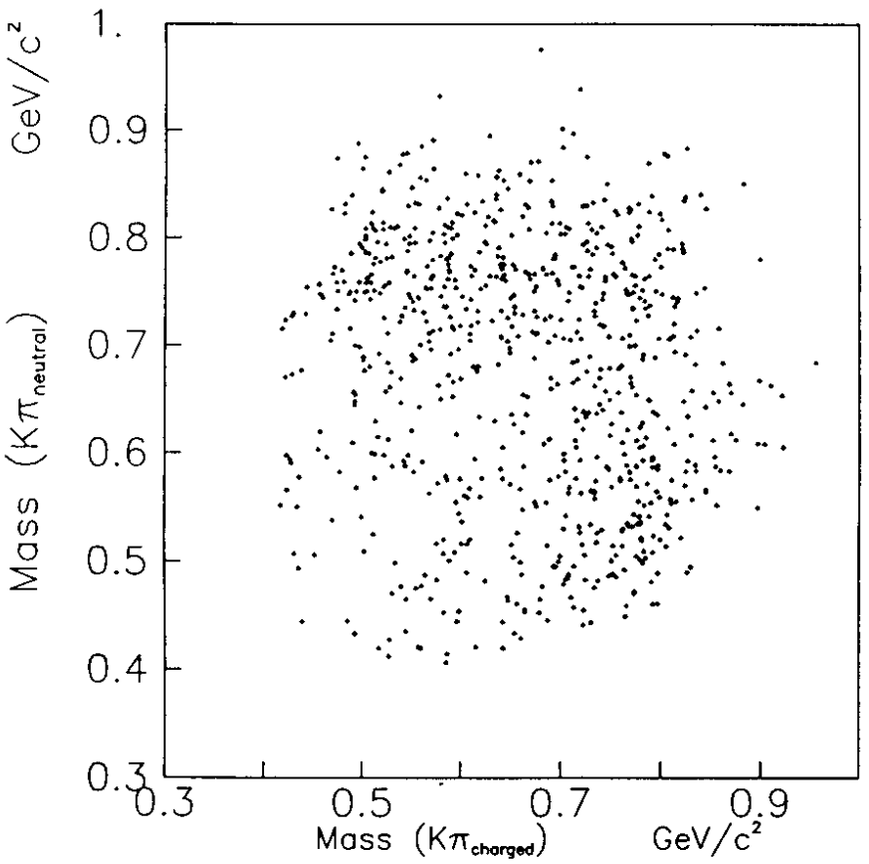
Mass ($K\pi_{neutral}$) GeV/c^2
Mass ($K\pi_{charged}$) GeV/c^2
1.
0.9
0.8
0.7
0.6
0.5
0.4
0.3
0.3
0.5
0.7
0.9

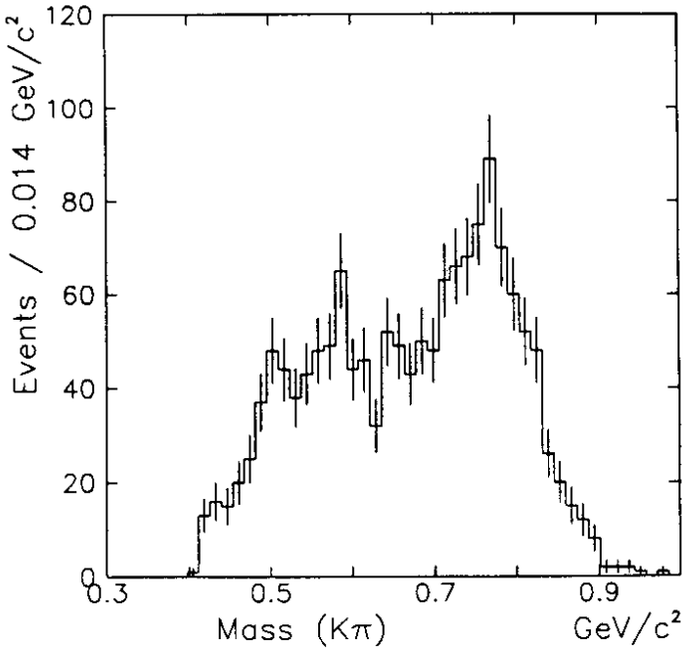
Events / 0.014 GeV/c^2
Mass ($K\pi$) GeV/c^2
120
100
80
60
40
20
0
0.3
0.5
0.7
0.9

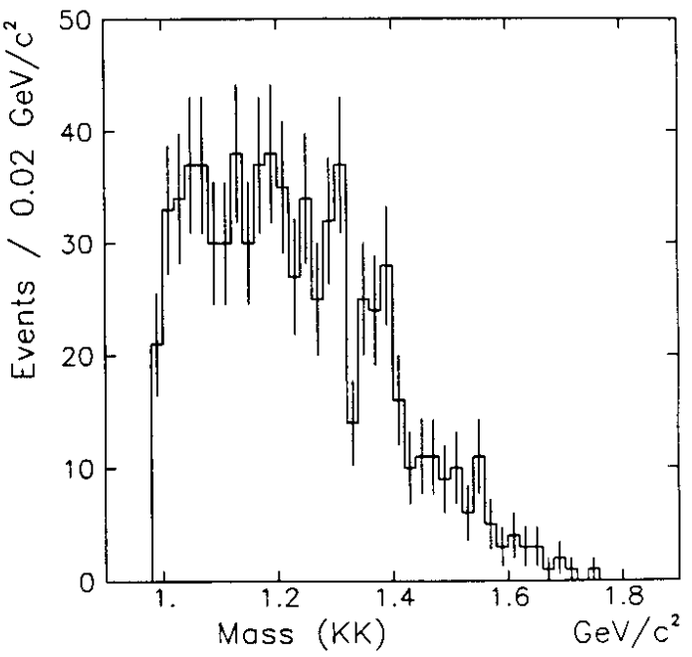
Events / 0.02 GeV/c^2
Mass (KK) GeV/c^2
50
40
30
20
10
0
1.
1.2
1.4
1.6
1.8

Fig.18

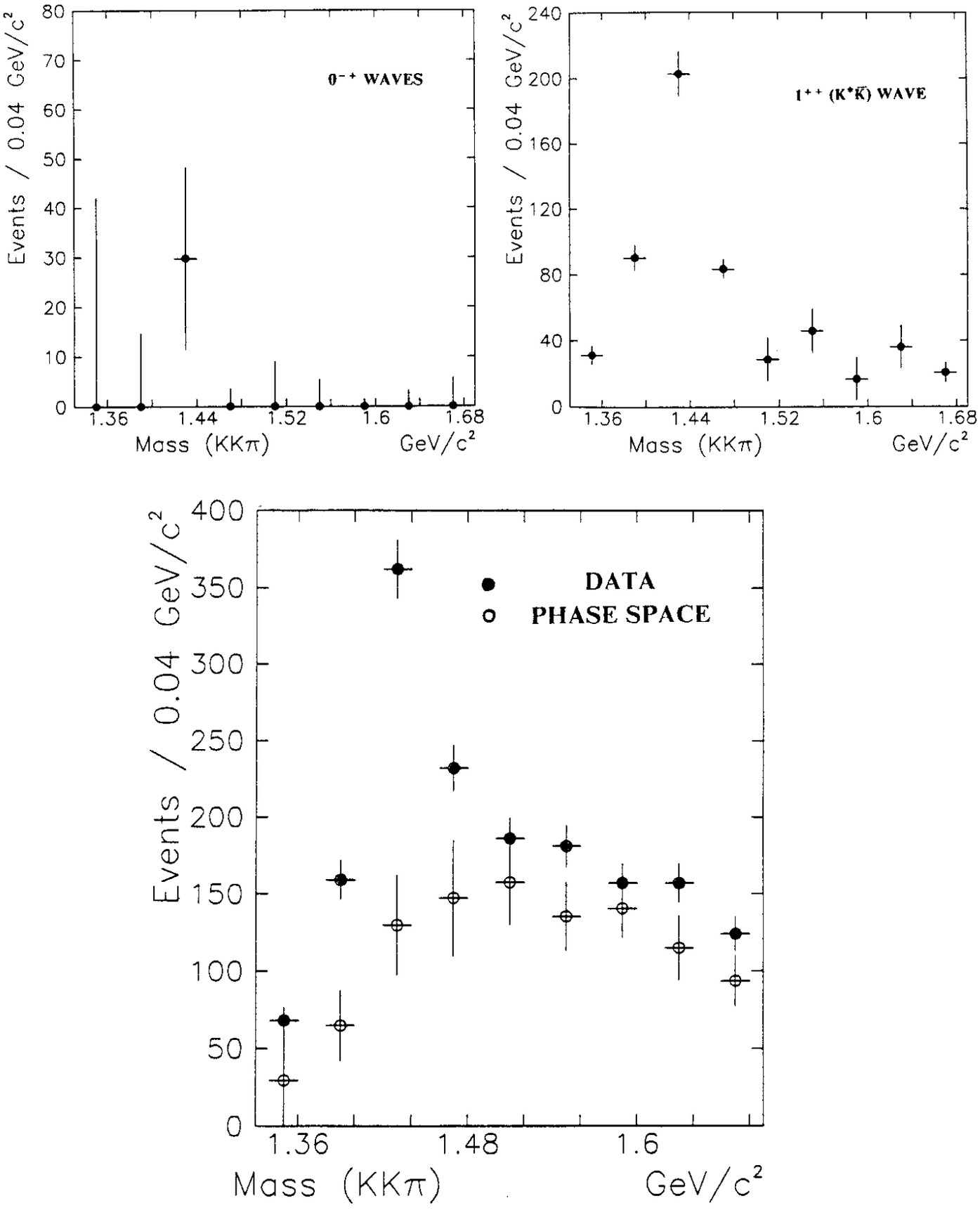
0^{-+} WAVES
1^{++} $(K^*\bar{K})$ WAVE
DATA
PHASE SPACE
Events / 0.04 GeV/c²
Mass (KKπ) GeV/c²
1.36
1.44
1.48
1.52
1.6
1.68

Fig.19

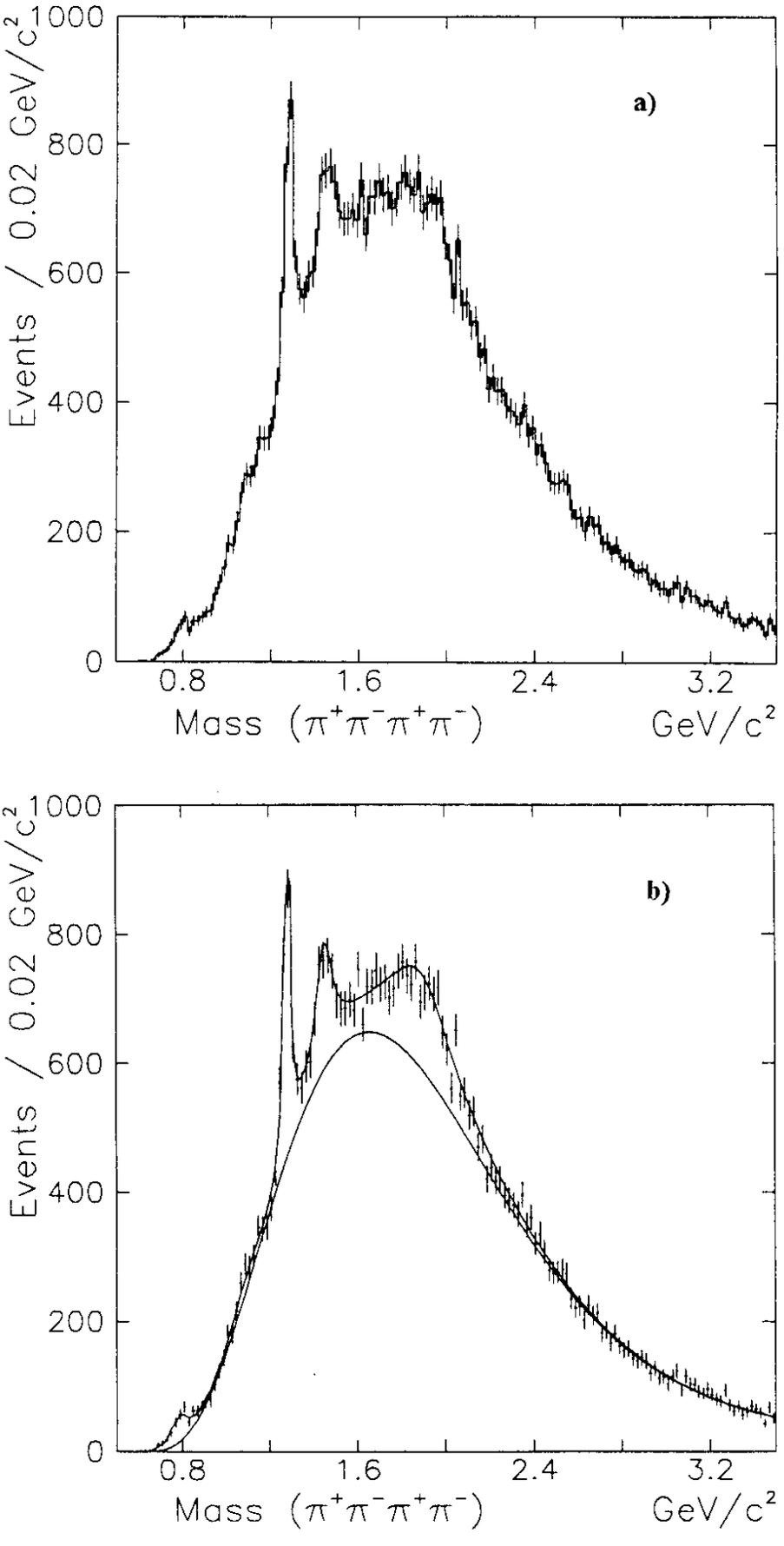
a)
b)
Events / 0.02 GeV/c²
1000
800
600
400
200
0
0.8
1.6
2.4
3.2
Mass $(\pi^+\pi^-\pi^+\pi^-)$
GeV/c²

Fig.20